

A Numerical Design of Marine Current for Predicting Velocity and Kinetic Energy

Parabelem Tinno Dolf Rompas^{*1}, Heindrich Taunamang², Ferry Johnny Sangari³

¹Departemen Pendidikan Teknologi Informasi dan Komunikasi, Universitas Negeri Manado, Kampus FT Unima, Tondano 95618, Indonesia, +62431322543

²Departemen Fisika, Universitas Negeri Manado, Kampus FMIPA Unima, Tondano 95618, Indonesia, +62431321845

³Departemen Pendidikan Teknik Elektro, Universitas Negeri Manado, Kampus FT Unima, Tondano 95618, Indonesia, +62431322543

*Corresponding author, e-mail: parabelemrompas@unima.ac.id

Abstract

One of marine current power plant equipment is turbine. In the design of marine current turbines required variables such as velocity and kinetic energy. This paper presents numerical study on a numerical design of marine current for predicting velocity and kinetic energy in the Bangka strait, North Sulawesi, Indonesia that developed from Yaxum/3D model. This study includes the simulation of velocity and kinetic energy distributions at low and high tide current conditions by two flow rates of 0.1 and 0.3 Sv respectively. The numerical method used to design computational program. Semi-implicit finite difference method used to 3D shallow water flow. It found distributions of velocity and kinetic energy at high tide current condition greater than low tide current condition. The future, these results will be developed in marine current power plant project in the Bangka strait, North Sulawesi, Indonesia.

Keywords: marine current velocity, kinetic energy, numerical design, Yaxum/3D

Copyright © 2017 Institute of Advanced Engineering and Science. All rights reserved.

1. Introduction

Velocity and kinetic energy of marine currents which are one of the renewable energy resources can be predicted by a numerical study that designed through a numerical model. Data obtained by the results of numerical computation can be used in the design of marine current turbines and feasibility studies in the construction of marine current power plant in the Bangka Strait, North Sulawesi, Indonesia in the future. Shevkar and Otari [1] have discussed tidal energy as tidal power that has potential for upcoming electricity generation. Erwandi et al [2] developed vertical axis marine current turbine in Indonesian Hydrodynamic Laboratory-Surabaya for tidal power plant. Also, they have employed to predict the strongest marine current at Larantuka strait between Flores and Adonara islands by using a numerical ocean modeling. Elbatran, et al., [3] have designed and developed the horizontal axis marine current turbine (HAMCT) for operating within Malaysian ocean in the current study. Soedibyo, et al., [4] have applied various renewable energy through modeling and simulation with using ANFIS in microgrid system.

The numerical solution in San Francisco Bay, California has conducted by Casulli and Cheng [5] who using the semi-implicit finite difference method. Gillibrand et al [6] have proposed numerical simulations which used the 3D shallow water equations derived from the RANS equations by using the hydrostatic assumption. Rodriguez-Cuevas, et al., [7] have been conducted a number of numerical experiments through test various turbulence models for shallow fluxes with recirculation of wakes produced by an island with a slight slope in their numerical simulations. Rompas and Manongko [8] proposed the study on the distributions of marine current velocity and kinetic energy in the Strait of Bunaken, North Sulawesi, Indonesia. The numerical solution of the shallow water equations on the sphere by using an efficient exponential time method has been presented by Gaudreault and Pudykiewicz [9]. Ramirez-Leon, et al., [10] developed the horizontal and vertical dispersion of salinity and temperature the YAXUM/3D baroclinic numerical model in the location of the Koombana bay. Ramirez-Leon, et al., [11] used the numerical model which solves the Navier-Stokes-Reynolds equations of

shallow water and energy equation for computing temperature variations. Chen [12] has been developed the free-surface correction (FSC) method, a semi-implicit, and 3-D finite difference model for free-surface flows through the numerical solution which was applied to the estuarine portion of the Alafia River in southwest Florida.

In this paper, we investigate the distributions of marine currents velocity and energy kinetic when low and high tide currents in the Bangka strait, North Sulawesi, Indonesia by a numerical design that developed from YAXUM/3D model. We develop the boundary conditions at the bottom, the surface of the water, the wall, and open boundary. Also, we calculate the kinetic energy from marine currents velocity.

Fundamental mathematics equation that used in the numerical model is the conservation of energy equation. It would express the variations in temperature, especially in account dissipation by friction, will ignore and temperature will later appear as a tracer only liable for the effects of buoyancy. Conservative of the fluid mass based on the following equation [5-6], [13-14].

$$\frac{\partial(\bar{U})}{\partial t} + \bar{U}\nabla\bar{U}) = \frac{1}{\rho} \text{div}(\underline{\sigma}) + \bar{g} + \bar{F} \quad (1)$$

Where ρ be the density of the fluid, and \bar{U} the velocity vector, whose components are U, V, W . ∇ is the tensor operator "nabla". $\bar{g} + \bar{F}$ is external forces where g is the constant gravitational acceleration and the other forces (Coriolis acceleration, etc.).

In this study, base on the decomposition of preceding Reynolds and under the assumptions of hydrostatic pressure, then conservative of the fluid mass become Realized Average Navier-Stokes (RANS) equations [14, 15]. The RANS equations were as a basic for the formulation of numerical model.

The domain of the Bangka strait is more complex of forms to free surface flows. Therefore, it needs limited. Some types of boundary conditions are required such as the boundary conditions at the bottom, the surface of the water, the wall, and open boundary. The first, at the bottom only horizontal velocity that could considered with used a Chezy formula [5]. At the surface, we used principally two conditions, the first is wind shear stresses in x -direction and the second is wind shear stresses in y -direction [12]. At the wall, we used the impermeable condition [13]. Finally, a condition of radiation and adaptive boundary condition that developed by Marchesiello, et al., [16] and Treguier, et al., [17] used at open boundary.

The turbulent model used dept-average formulation from Stansby [18] as defined follow:

$$v_t = \left(l_h^4 \left[2 \left(\frac{\partial \bar{u}}{\partial x} \right)^2 + 2 \left(\frac{\partial \bar{v}}{\partial y} \right)^2 + \left(\frac{\partial \bar{v}}{\partial x} + \frac{\partial \bar{u}}{\partial y} \right)^2 \right] + (\gamma \bar{u}_f h)^2 \right)^{1/2} \quad (2)$$

Where the friction velocity $\bar{u}_f = \sqrt{|\tau_b|/\rho}$ with ρ is water density and bed shear stress

$\tau_b = \sqrt{\tau_{bx}^2 + \tau_{by}^2}$ where $(\tau_{bx}, \tau_{by}) = C_f \rho (\bar{u}, \bar{v}) \sqrt{\bar{u}^2 + \bar{v}^2}$ with $C_f = 0.0559 \text{Re}_h^{-0.25}$ is friction

coefficient of the Blasius formula where the depth Reynolds number $\text{Re}_h = (\sqrt{\bar{u}^2 + \bar{v}^2})h/\nu$, and γ is the Elder constant about 0.067 which are the depth-averaged vertical mixing, and the horizontal mixing length $l_h = \beta\lambda h$ where λ is a boundary layer constant ($\lambda=0.09$), h is water depth and $\beta=l_h/l_v$ is the constant from result comparison with experiment.

The numerical equations that used in this study were results developing from mathematical equations. Also, from the results of modification of the YAXUM/3D model that used by [7-8], [10-11]. In the numerical model, we used semi-implicit finite difference method for the numerical solution of the three-dimensional Equation (1) in the computation of shallow water flows [5, 14].

The velocities in x, y , and z directions, we used the equations which a general semi-implicit discretization of the momentum equations and we can written in the more compact matrix form as [5, 14]

$$A_{i+1/2,j}^n \mathbf{U}_{i+1/2,j}^{n+1} = \mathbf{G}_{i+1/2,j}^n - g \frac{\Delta t}{\Delta x} (\eta_{i+1,j}^{n+1} - \eta_{i,j}^{n+1}) \Delta \mathbf{Z}_{i+1/2,j}^n \tag{3}$$

$$A_{i,j+1/2}^n \mathbf{V}_{i,j+1/2}^{n+1} = \mathbf{G}_{i,j+1/2}^n - g \frac{\Delta t}{\Delta y} (\eta_{i,j+1}^{n+1} - \eta_{i,j}^{n+1}) \Delta \mathbf{Z}_{i,j+1/2}^n \tag{4}$$

2. Research Method

The geographical location of the Bangka Strait is from 125 ° 04'40 "E to 125 ° 11'18" E and from 1 ° 41'25 "N to 1 ° 44'03" N which consist of islands of Talise, Kinabuhutan, Ganges, Tindila, Lehaga, and Sulawesi. In the east, there are the Maluku Sea and Pacific oceans, and to the west is the Sulawesi Sea (see Figure 2). In addition, there are two of the current circulations (bidirectional) in the Bangka strait i.e. low tide currents and high tide currents.

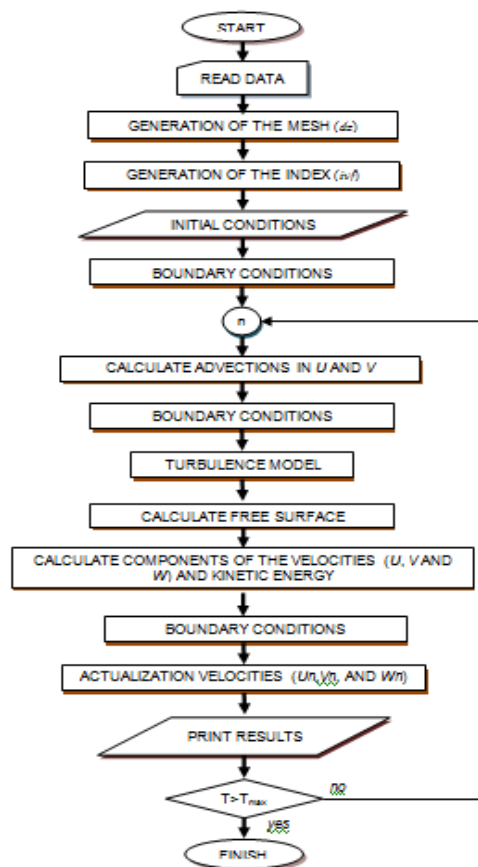


Figure 1. Flowchart of the numerical design

The methods used survey, observation, and measurement in the Bangka strait. The data of seawater density conducted measurement in the Bangka strait. The data of width and depth in the strait collected from the map of Bangka strait and its depth of the sea. Problem solving of the study used a numerical model. The solution of a numerical model we take the case in the Bangka strait for calculating the velocities of \bar{u} , \bar{v} and \bar{w} respectively, we can explain step by step (Figure 1) as the first is the beginning of computation with start. Then, the read data that using the all of parameters in the numerical equations and time of calculating until time maximum for doing iteration. Next step, generation of the mesh such as horizontal and vertical meshes and then continue to the process generating the index such as generate the layers of vertical axis (depth) and boundary layers. The next process, it makes the initial

conditions of velocities and seawater surface elevation and the boundary conditions. Then, step in the start of iteration process until maximum iteration that the beginning with calculate advectons in \bar{u} and \bar{v} , which are the processes for calculating advectons of horizontal velocities, and then it makes the boundary conditions again in the Bangka strait. Next, it calculates the turbulence and the free surface that using a linear five-diagonal system. Then, it calculates components of velocities in horizontal and vertical directions and kinetic energy. Next, it makes back the boundary conditions and actualization velocities. Then, it prints the results of velocities and kinetic energy. Finally, the process to do execution which if the iteration has been greater than maximum iteration, then calculation to finish but if no, then to be continue calculate advectons in \bar{u} and \bar{v} again.

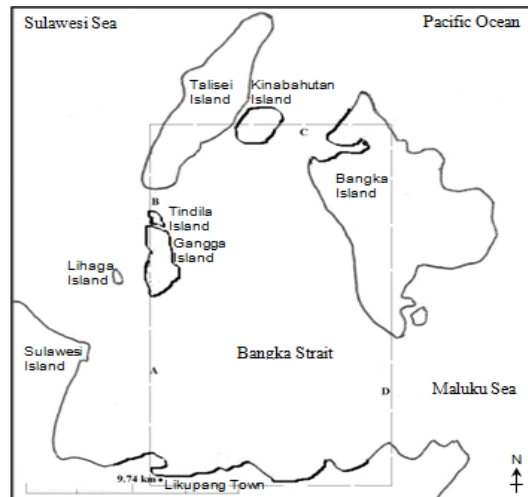


Figure 2. Location of numerical study

Table 1. Numerical Parameters for 3D-Simulations

Parameters	Value	Parameters	Value
g	9.81 m s ⁻²	$\rho_{seawater}$	1024 kg/m ³
Cz	48	Δx	60 m
τ_o	2 days	Δy	60 m
τ_i	1 day	Δz	20 m
flow rate	variable	Δt	1 sec

In Table 1, there are two flow rates that determined i.e. 0.1 Sv and 0.3 Sv (1 Sv = 1 Sverdrup = 10⁶ m³/s [19]). τ_o and τ_i are relaxation timescales at outflow and inflow conditions respectively [15, 16]. Cz is Chezy coefficient and $\rho_{seawater}$ is density of seawater. Δx , Δy , Δz , and Δt are space step in x , y , and z directions, and time step respectively.

3. Results and Analysis

Figure 3-9 showed the results of numerical simulation. We can see Figure 3 and 4 that in the form of simulations i.e. 2D-simulations at seawater column of 20 m when low tide currents and high tide currents. Figure 3 shows distributions of velocities and current threads at seawater column when low tide currents. Generally, seawater enters from section A and B where current flows from section A and go to section D and a small part flow to section C which previous rotate form two eddies like elliptic diameter at centre between Gangga and Bangka Islands. On the other side, current enter in section B flow to section C which previous form eddy in north area near Talise Island and a small part flow to section D which previous form small maelstrom like diameter between Gangga and Bangka islands. On the contrary, when high tide current (Figure 4), current enters from section D go to section A and a small part flow to section B which previous happened eddy at center east area near Bangka Island whereas current from section

C go to section B which previous form eddy like elliptical diameter at north area near Talise Island and a small part of the other current go to south side of Gangga Island at section A.

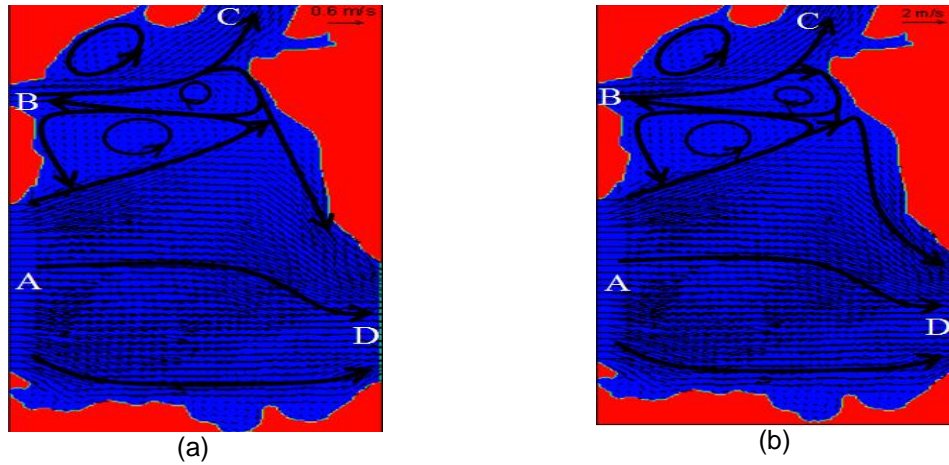


Figure 3. Simulations (2D) of marine current velocities and current threads at seawater column of 20 m when low tide currents at 0.1 Sv (a) and 0.3 Sv (b)

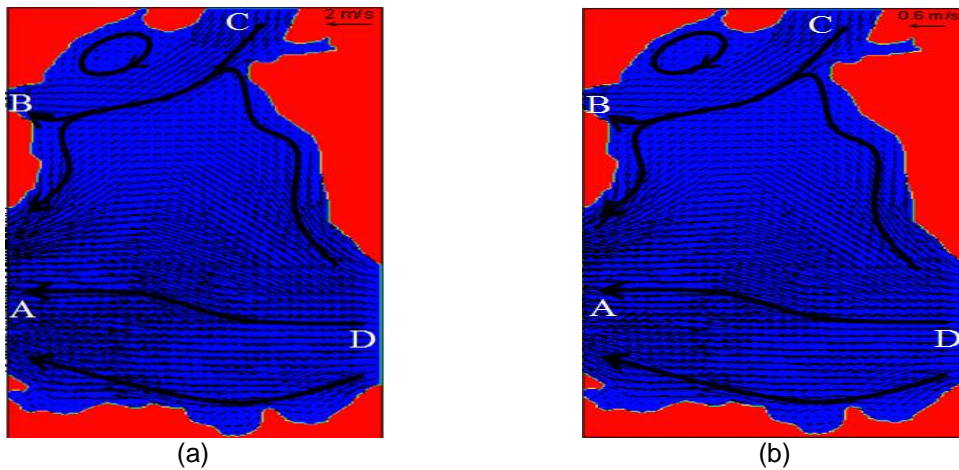


Figure 4. Simulations (2D) of marine current velocities and current threads at seawater column of 20 m when high tide currents at 0.1 Sv (a) and 0.3 Sv (b)

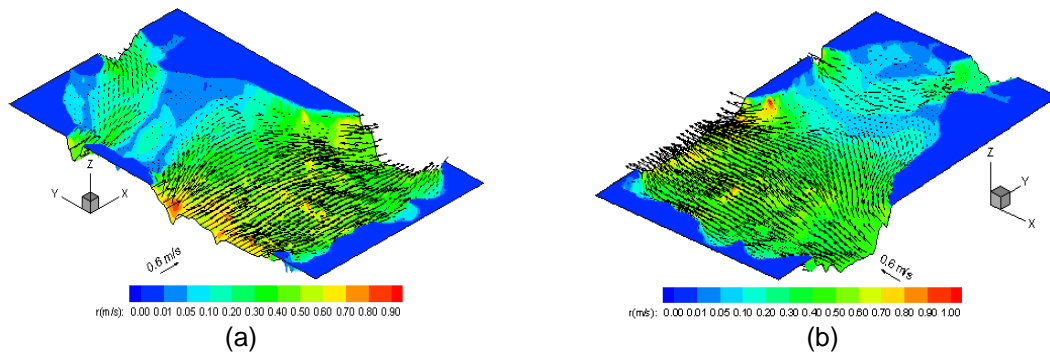


Figure 5. Simulated (3D) of marine current velocities distribution at seawater column of 20 m when low (a) and high (b) tide currents at 0.1 Sv

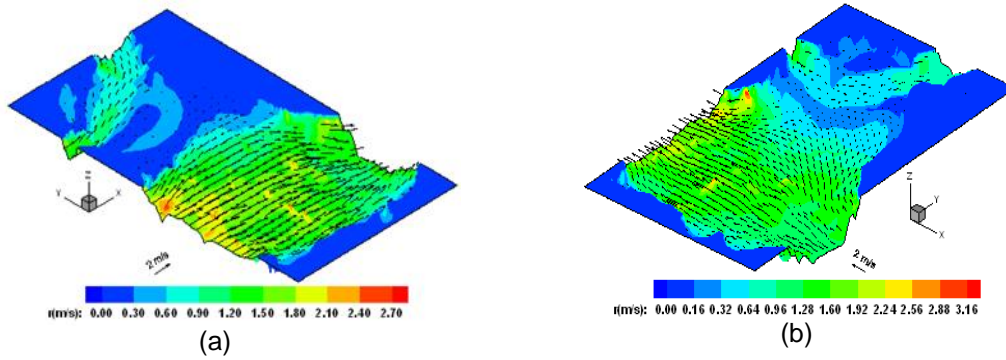


Figure 6. Simulated (3D) of marine current velocities distribution at seawater column of 20 m when low (a) and high (b) tide currents at 0.3 Sv

Figure 5 and 6 show simulated (3D) of marine current velocities distribution at seawater column of 20 m when low (a) and high (b) tide currents at 0.1 and 0.3 Sv respectively. When high tide currents, the volume of seawater passing through the area was so large which is the result of a combination of direction section C and D (see also Figure 4). Whereas when low tide current (see bottom centre area) flow only from section C. The currents were so strong in the top of section A. It is because not only so large volumes of seawater but also depth of 6 m.

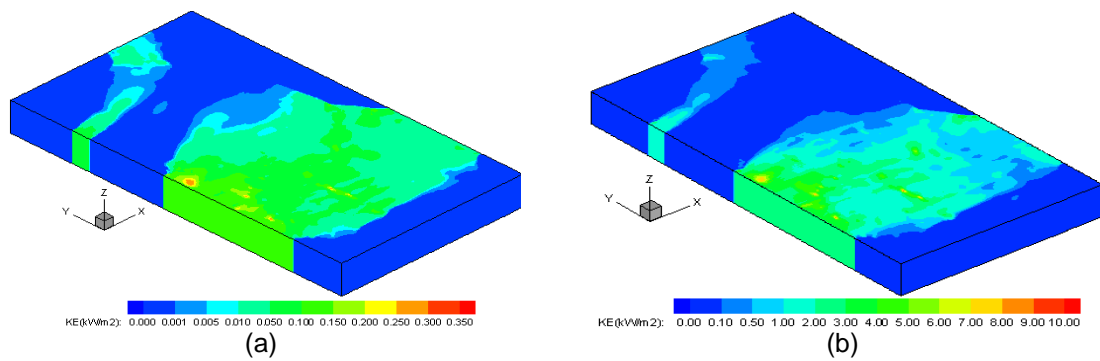


Figure 7. Simulated (3D) distributions of the kinetic energy at seawater column of 20 m when low tide currents at flow rates of 0.1 Sv (a) and 0.3 Sv (b)

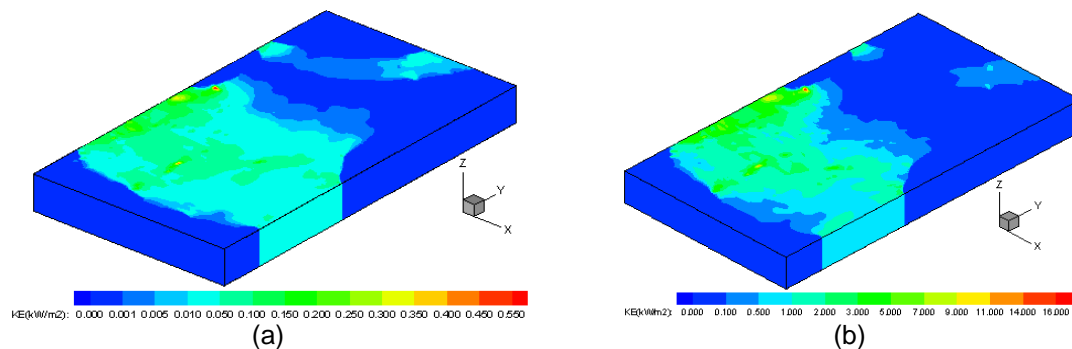


Figure 8. Simulated (3D) distributions of the kinetic energy at seawater column of 20 m when high tide currents at flow rates of 0.1 Sv (a) and 0.3 Sv (b)

Figure 9 shows velocity vector field and kinetic energy distributions at seawater column of 20 m when low (a) and high (b) tide currents at 0.3 Sv in the Bangka strait. In the centre area of strait (see Tables 2 and 3), we can see that the values of velocity can be used to design profile of the marine current turbine. The results if we compare the results of marine currents numerical simulation in the Bunaken Starit that presented by [6] which at flow rate of 1 Sv, the average velocities at enter of Bunaken Strait is 1.46 m/s when low tide currents and 0.85 m/s when high tide currents. It shows difference in the boundary conditions. We can also compare with seeing the results of discussions by [5, 7], [10-12]. Besides, this area is suited installed turbines for marine current power plant and ideal, it has velocities of current two directions (minimum bidirectional) of 2 m/s or more, one way is minimum 1.2-1.5 m/s [13, 20]. Also, the depth not less than 15 m and the more than 40-50 m, the construction near the beach so that energy can be supplied at low cost, the area is spacious enough for more than one turbine installation, and no the area of sea transport and fishing.

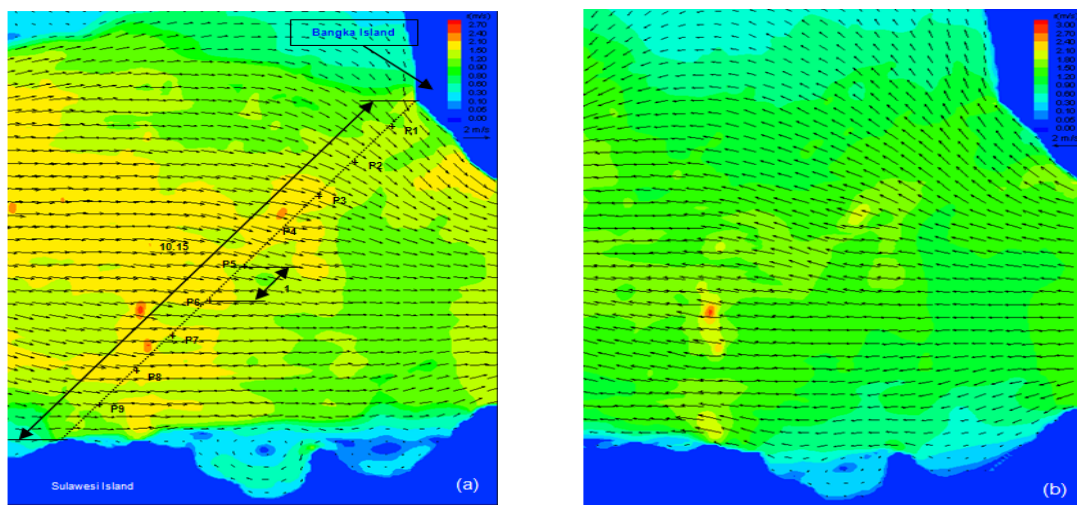


Figure 9. Velocity vector field and kinetic energy distributions at seawater column of 20 m when low (a) and high (b) tide currents at 0.3 Sv in the Bangka strait

Figure 5 shows 3D-simulation of the velocity distributions at seawater column of 20 m when low and high tide currents at 0.1 Sv. Same as Figure 5, in Figure 6 shows flow rate of 0.3 Sv. Maximal velocities are predominated at around section A, whereas in the center of Bangka strait which average velocity is 1.45 m/s at average depth of 21.4 m (we can be seen in Figure 9 and Table 2 and 3). It also obtained average kinetic energy is 1.6 kW/m² (see Figure 7 and 8, and also Table 2 and 3). Tidal power energy (kinetic energy) can be predictable if compared to other energy sources [1, 3]. Figure 5-9 are show that the velocity and the kinetic energy when low and high tide currents almost equal.

Table 2. Values of velocity vector fields and the kinetic energy (KE) at flow rate of 0.3 Sv when low tide currents

POINT	\bar{u} m/s	\bar{v} m/s	\bar{w} m/s	Direction degree	v m/s	KE kW/m ²	Depth m
P1	0.76	-0.97	0.00	308	1.24	0.97	-22
P2	1.07	-0.81	-0.01	323	1.34	1.24	-21
P3	1.38	-0.67	-0.01	334	1.53	1.85	-23
P4	1.59	-0.33	0.00	348	1.63	2.22	-22
P5	1.31	-0.35	-0.01	345	1.36	1.29	-28
P6	1.52	-0.18	0.00	353	1.53	1.83	-20
P7	1.43	-0.12	0.00	355	1.43	1.51	-20
P8	1.59	0.00	0.00	0	1.59	2.07	-20
P9	1.27	-0.04	0.00	358	1.27	1.04	-17

Table 3. Values of velocity vector fields and kinetic energy (KE) when high tide currents at flow rate of 0.3 Sv

POINT	\bar{u} m/s	\bar{v} m/s	\bar{w} m/s	Direction degree	v m/s	KE kW/m ²	Depth m
P1	-0.61	1.10	0.00	119	1.26	1.02	-22
P2	-1.02	1.06	0.01	134	1.47	1.64	-21
P3	-1.28	0.82	0.01	147	1.53	1.82	-23
P4	-1.46	0.28	0.00	169	1.48	1.67	-22
P5	-1.43	0.50	0.01	161	1.52	1.78	-28
P6	-1.46	0.22	0.00	171	1.47	1.64	-20
P7	-1.35	0.30	0.00	167	1.38	1.35	-20
P8	-1.59	0.14	0.00	175	1.60	2.10	-20
P9	-1.49	0.13	0.00	175	1.50	1.72	-17

4. Conclusion

We successfully obtained the velocity and kinetic energy distributions of marine currents at seawater column of 20 m in the Bangka strait, North Sulawesi, Indonesia by the 2D and 3D numerical models. The velocities of marine current at seawater column when low and high tide currents which the maximum happened at 0.1 Sv were 0.9 and 1.0 m/s respectively, while at 0.3 Sv were 2.7 and 3.16 m/s respectively. Whereas, the kinetic energy maximum at 0.1 Sv were 0.35 and 10 kW/m² respectively when low tide currents, while when high tide currents at 0.3 Sv were 0.55 and 16 kW/m² respectively. The results will be a product in analyzing the potential kinetic energy, which can used to design profile of turbines for marine currents power plant in the Bangka strait North Sulawesi, Indonesia.

References

- [1] Shevkar SS, Otari KA. Tidal Energy Harvesting. *International Journal of Science, Engineering and Technology Research (IJSETR)*. 2015; 4(4): 990-994.
- [2] Erwandi, K Afian, Sasoko P, Rina, Wijanarko B, Marta E, Rahuna D. *Vertical Axis Marine Current Turbine Development in Indonesian Hydrodynamic Laboratory-Surabaya for Tidal Power Plant*. International Conference and Exhibition on Sustainable Energy and Advanced Materials (ICE SEAM 2011). Solo. 2011; 1: 15-23.
- [3] Elbatran AHA, Yaacob OB, Ahmed YM, Abdullah FB. Augmented Diffuser for Horizontal Axis Marine Current Turbine. *International Journal of Power Electronics and Drive System (IJPEDS)*. 2016; 7(1): 235-245.
- [4] Soedibyo, Murdianto FD, Suyanto, Ashari M, Penangsang O. Modeling and Simulation of MPPT-SEPIC Combined Bidirectional Control Inverse KY Converter Using ANFIS in Microgrid System. *Indonesian Journal of Electrical Engineering and Computer Science*. 2016; 1(2): 264.
- [5] Casulli V, Cheng RT. Semi-implicit Finite Difference Methods for Three-Dimensional Shallow Water Flow. *International Journal for Numerical Methods in Fluids*. 1992; 15: 629-648.
- [6] Gillibrand PA, Walters RA, McIlvenny J. Numerical Simulations of the Effects of a Tidal Turbine Array on Near-Bed Velocity and Local Bed Shear Stress. *Energies*. 2016; 9(852): 5-8.
- [7] Rodriguez-Cuevas C, Couder-Castaneda C, Flores-Mendez E, Herrera-Diaz IE, Cisneros-Almazan R. Modelling Shallow Water Wakes Using a Hybrid Turbulence Model. *Journal of Applied Mathematics*. 2014; 2014: 2-5.
- [8] Rompas PT, Manongko JDI. Numerical Simulation of Marine Currents in the Bunaken Strait, North Sulawesi, Indonesia. *IOP Conference Series: Materials Science and Engineering*. 2016; 128: 1-7.
- [9] Gaudreault S, Pudykiewicz JA. An Efficient Exponential Time Integration for the Numerical Solution of the Shallow Water Equations on the Sphere. *Journal of Computational Physic*. 2016; 322: 827-848.
- [10] Ramirez-Leon H, Barrios-Pina HA, Rodriguez-Cuevas C, Couder-Castaneda C. Baroclinic Mathematical Modeling of Fresh Water Plumes in the Interaction River-Sea. *International Journal of Numerical Analysis and Modeling*. 2005; 2: 1-14.
- [11] Ramirez-Leon H, Couder-Castaneda C, Herrera-Diaz IE, Barrios-Pina HA. Modelacion Numerica de la Descarga Termica de la Central Nucleoelectrica Laguna Verde. *Revista Internacional de Metodos Numericos para Calculo y Diseno en Ingenieria*. 2013; 29(2): 114-121.
- [12] Chen XJ. A Free-Surface Correction Method for Simulating Shallow Water Flows. *Journal Computational Physics*. 2003; 189: 557-578.
- [13] Fraenkel PL. *New Development in Tidal and Wave Power Technologies*. Presented at Towards a renewable future: Silver Jubilee Conference. Brighton. 1999: 156.

- [14] Hervouet JM. Hydrodynamics of Free Surface Flows: Modelling with the Finite Element Method. England: John Willey & Sons. 2007: 341.
- [15] Broomans P. Numerical Accuracy in Solution of the Shallow-Water Equations. Master thesis. TU Delft & WL, Delft Hydraulics; 2003.
- [16] Marchesiello P, McWilliams JC, Shchepetkin A. Open Boundary Conditions for Long-term Integration of Regional Oceanic Models. *Ocean Modelling*. 2001; 3: 4-7.
- [17] Treguier AM, Barnier B, De Miranda AP, Molines JM, Grima N, Imbard M, Madec G, Messenger C, Reynaud T, Michel S. An Eddy-Permitting Model of the Atlantic Circulation: Evaluating Open Boundary Condition. *Journal of Geophysical Research*. 2001; 106(C10): 22,117-22,118.
- [18] Stansby PK. Limitations of Depth-Averaged Modeling for Shallow Wakes. *Journal of Hydraulic Engineering*. 2006; 132(7): 737-740.
- [19] Siedler G, Church J, Gould J. Ocean Circulation and Climate: Observing and Modelling the Global Ocean. San Diego: Academic Press. 2001: 715.
- [20] Fraenkel PL. Power from Marine Currents, Proceedings of the Institution of Mechanical Engineers: Part A. *Journal of Power and Energy*. 2002; 216(1): 1-14.